Appendix B

Radiation Damage and Curing

The transparency of lead-glass decreases as it is irradiated. Radiation damage of lead-glass leads to a *yellowing* or *darkening* of the lead-glass. The coloring of the lead-glass is caused by creation of color centers or by the development and growth of absorption bands. The absorption bands decrease the amount of Čerenkov light which reaches the photomultiplier tube and, therefore, decrease the signal.

A spectrophotometer which measures the transmittance or absorption of materials has been used to monitor radiation damage. Several F2 lead-glass sample pieces, $\approx 10 \times 2 \times 2$ cm^3 with only the two small end faces parallel and polished, have been used to monitor the radiation damage/exposure of the central calorimeter. The calorimeter's lead-glass blocks have not been used directly since they are contained within the wedge shells and are inaccessible. Using the smaller lead-glass sample pieces, the spectrophotometer is used in its normal configuration (not as described in Appendix A). In addition to the lead-glass samples placed about the calorimeter during the running, two pieces have been placed near the debuncher ring's injection kicker magnet for a short period of time.

Placement Comment		Azimuthal Angle	Distance (cm)
Upstream	+x-axis	5°	60
Upstream	+y-axis	90°	75
Upstream	−x-axis	175°	75
Upstream	−y-axis	270°	130
Downstream	+x-axis	345°	120
Downstream	+y-axis	85°	135
Downstream	−x-axis	195°	105
Downstream	−y-axis	265°	130

Table B.1: The azimuthal angles and radial distance from beam pipe of the lead-glass samples about the calorimeter.

B.1 Placement of Lead-glass Samples

The lead-glass samples have been present constantly about the central calorimeter whenever there has been beam in the $\bar{p}$ source. Twenty-four samples have been separated into sets of three and placed at eight locations about the calorimeter. Each lead-glass sample is wrapped individually in black paper. The locations have been essentially along the experiment's positive and negative x and y axes (the z-axis is along the $\bar{p}$ direction and the y-axis is pointing upward) upstream and downstream of the calorimeter. Table B.1 shows the approximate azimuthal angles and the radial distance from the beam pipe for the eight sets. The approximate polar angles at the upstream end near the interaction point are 80° for the sets along the x-axis and between 72° and 75° for the sets along the y-axis. The downstream samples have been connected to the central calorimeter cable support apparatus located 265 cm downstream of the interaction point.

Two samples were placed near the debuncher ring's injection magnet, with no shielding, during $\bar{p}$ source studies conducted in December 1990. In between the debuncher and accumulator rings near the E760 experimental area, concrete blocks provide shielding for the detector. The placement of the shielding intercepts particles coming from the $\bar{p}$ target area via the transport line and shields against radiation produced at the nearby kicker magnets. Previous to the start of the experiment, these were the expected radiation sources for E760.

B.2 Radiation Exposure

Several radiation monitors have also been placed about the calorimeter to try to measure the radiation dosage. The radiation monitors vary in type but all are connected to a visual readout system in the E760 counting room. Only two of the radiation monitors have been continually attached to the central calorimeter. The $\bar{p}$ source has operated for three different periods over two years with the central calorimeter present; the radiation dosages received by the calorimeter according to the two monitors are shown in table B.2. The two fixed target time periods had different shielding arrangements and different injection line collimator settings; additionally, the injection line tuning improved with time. During the $\bar{p}$ source studies, the E760 detector was removed from the beam line and moved as far away as possible within the experimental area from the debuncher and accumulator beam lines, however, the shielding was also removed and the collimators were opened wide. During data taking,

Time Period	Dosage (rad)
Fixed target run 1990 (May – September)	$\approx$ 70 rad
Studies of the $\bar{p}$ source (December 1990)	$\approx$ 30 rad
Fixed target run 1991 (June – January)	$\approx$ 80 rad

Table B.2: The radiation dosages, according to monitors, that the central calorimeter received in the $\bar{p}$ source.

when the gas jet is operating, the radiation monitors showed small radiation doses as compared to doses during stacking (the collection of $\bar{p}$'s).

A separate radiation monitor was placed near the kicker magnet when the two samples were in place during the December 1990 $\bar{p}$ source studies. This monitor, a propane gas ion chamber, was operated in what is called *neutron mode*, which is a factor of ten more sensitive to charged particles than neutral particles; the neutron mode assumes that the radiation does not consist of charged particles. The nature of the radiation is unknown and therefore the dosage determined from the monitor may be an over estimate. The monitor measured a dosage of 1200 rad before failing. Estimating from other radiation monitors in the area, the two samples received an additional 1000 to 2000 rad.

B.3 Radiation Damage Analysis

The transmission spectra of the lead-glass samples were made and recorded by an HP8451A spectrophotometer before exposing them to radiation. One spectrum is shown in figure B.1 along with a spectrum from one of the 50 cm long lead-glass

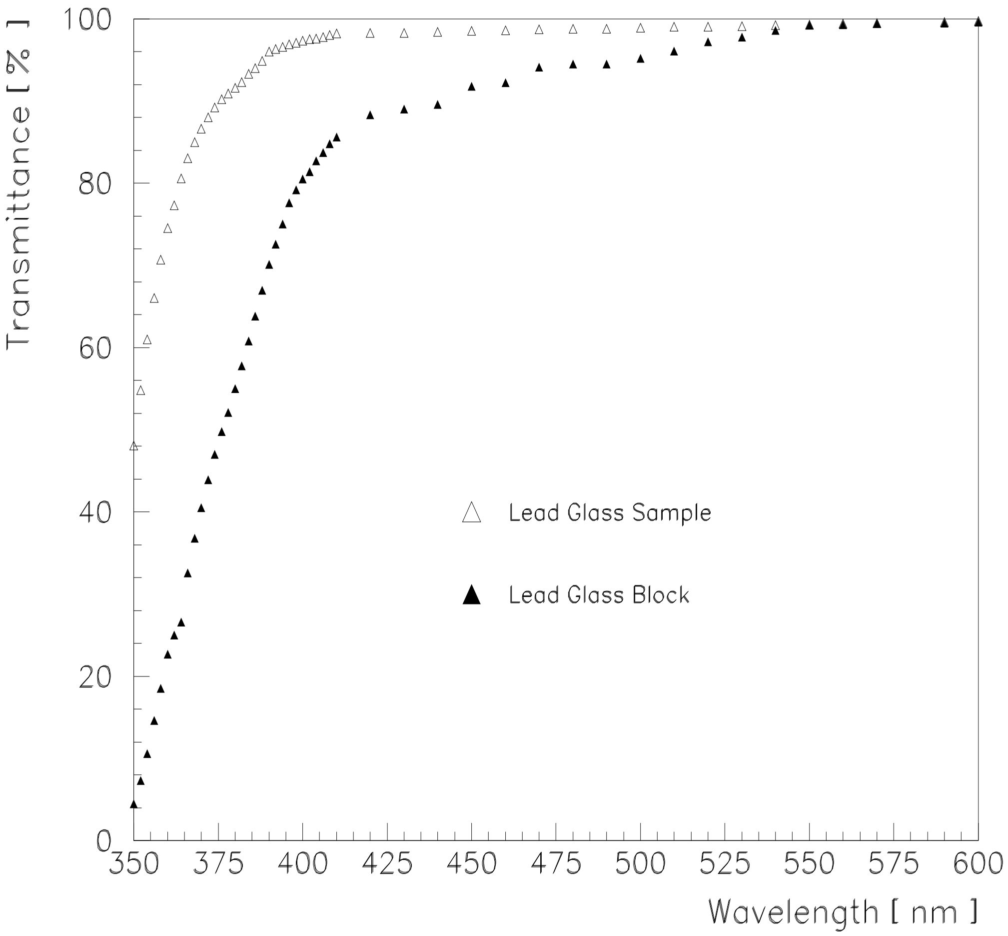

Figure B.1: A lead-glass sample's transmission spectrum and a 50 cm long lead-glass block spectrum.

blocks. The twenty-four lead-glass samples' transmittances have been re-measured after each time period as described in table B.2. None of the transmission spectra show any change, outside of the spectrophotometer's intrinsic error, from the original spectrum for the lead-glass samples that were located about the central calorimeter. The spectrophotometer's transmission measurement error for a 2 nm wavelength band interval is 2%. A 2% change in the transmittance of a small lead-glass sample

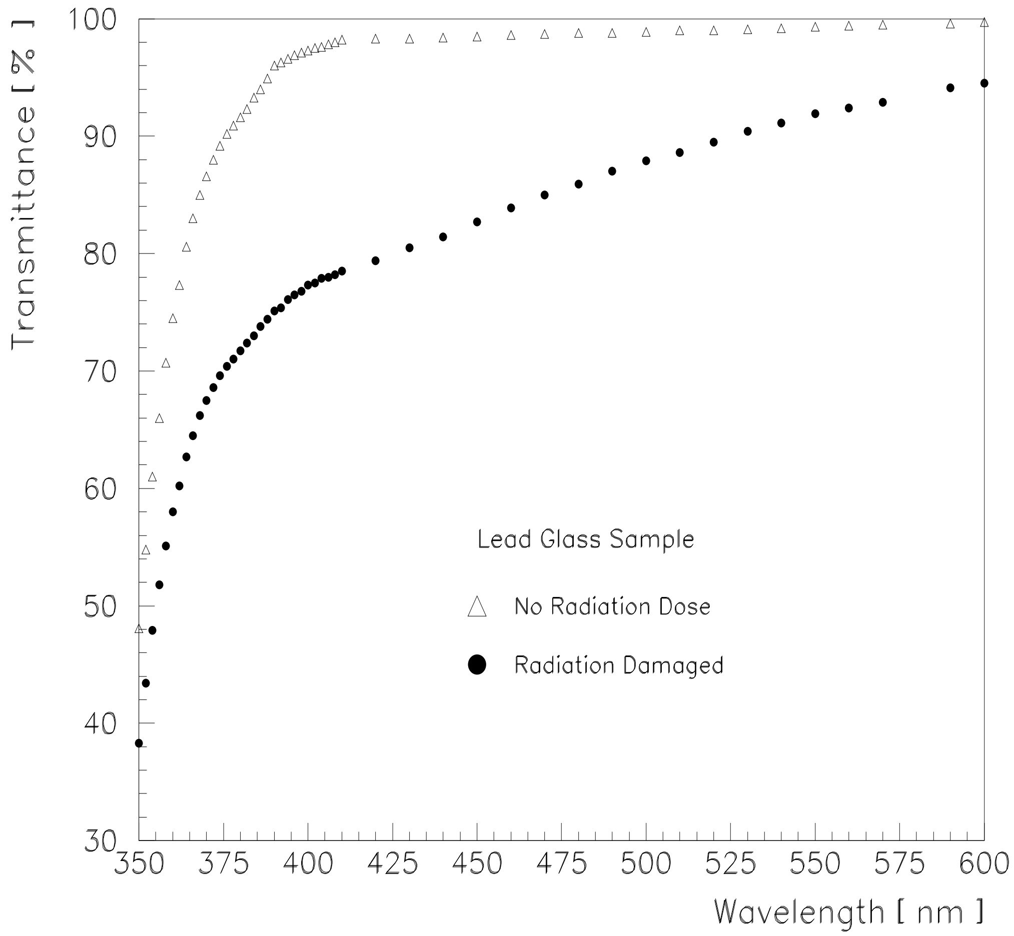

Figure B.2: The transmission spectra of one of the lead-glass samples before and after being placed near the debuncher ring's kicker magnet showing the affect of radiation damage.

corresponds to 10% change in the transmittance of a lead-glass block. The absorption of the flashlamp light would correspondingly change the flashlamp response by 20% since the light has to travel the block length twice. As stated in section 4.4.1, there has been no measureble decrease of the flashlamp response attributed to radiation damage. The lead-glass samples about the calorimeter agree with the flashlamp responses.

However, the two samples which were exposed to the larger radiation dose have shown radiation damage. Figure B.2 shows the radiation damage to the transmission spectrum; the original transmission spectrum is shown for comparison. The radiation damage affects the ultraviolet wavelengths more than the rest of the spectrum. Visually, the samples were darker and slightly brown.

The radiation dose can also be estimated another way. Kirsebom and Sollie [84] have parameterized the transmission properties of F2 lead-glass for absorbed doses, D, up to 5000 rad. The radiational absorption is defined

$$a(\lambda, D) = 1 - \frac{T(\lambda, D, x = 1\mathrm{cm})}{T_o(\lambda)}, \tag{B.1}$$

where $T_o(\lambda)$ is the non-irradiated transmittance $T(\lambda, D = 0 \text{ rad}, x = 1 \text{ cm})$. The parameterization found by Kirsebom and Sollie is

$$a(\lambda, D) = 1 - e^{-\mu(\lambda)D}, \tag{B.2}$$

where $\mu(\lambda)$ is experimentally determined. The transmittance through x cm of lead-glass is

$$T(\lambda, D, x) = [T(\lambda, D, x = 1\mathrm{cm})]^x \tag{B.3}$$

and substituting in appropriately the transmittance is

$$T(\lambda, D, x) = \left[T_o(\lambda)e^{-\mu(\lambda)D}\right]^x. \tag{B.4}$$

Several values of μ for several representative wavelengths have been determined by Kirsebom and Sollie. Using these values for $\mu(\lambda)$ and the transmission spectra

Wavelength (nm)	μ (10^{-6})	Calculated Dose (rad) Sample 1	Sample 2
350	40.7	434	490
400	31.8	692	622
450	21.6	782	660
500	13.3	831	670
600	5.1	652	544

Table B.3: The calculated radiation dose for the two lead-glass samples using $\mu(\lambda)$ values determined by Kiresbom and Sollie [84].

before and after irradiation, a calculated radiation dose can be determined:

$$D = \frac{1}{\mu(\lambda)x} \ln\left(\frac{T_x(\lambda)}{T(\lambda, D, x)}\right), \tag{B.5}$$

where $T_x = [T_o]^x$; the measured spectra are always for the transmittance through x cm of lead-glass. Table B.3 shows the calculated doses at the various wavelengths for the two lead-glass samples; the μ parameter is also shown. The radiation dosage appears to be between 600 and 700 rad and disagrees with the radiation monitor determination. Several explanations are possible for the discrepancy of a factor of 2 (the radiation monitor result before failure) to 5 (the largest extrapolated dosage). A basic reason could be that the F2 lead-glasses are not the same; however, one would not expect such a large difference. Another possible explanation is that the radiation monitors have overestimated the dosage since the nature of the radiation is unknown. A last possible explanation is that instant *bleaching*, or curing, of the the lead-glass occurs when exposed to light. The lead-glass samples were exposed to artificial lights while being unwrapped and placed in the spectrophotometer's sample compartment before a transmission spectrum was taken. The most reasonable explanation is that the radiation monitors have overestimated the radiation dosage.

λ (nm)	μ (10^{-6}) Sample 1 1200 rad	2000 rad	3000 rad	Sample 2 1200 rad	2000 rad	3000 rad
350	16.1	9.65	6.42	16.6	9.96	6.64
400	18.3	11.0	7.34	16.3	9.76	6.52
450	14.1	8.45	5.62	11.9	7.12	4.75
500	9.16	5.50	3.67	7.42	4.46	2.97
600	2.76	1.66	1.11	2.31	1.38	0.92

Table B.4: The calculated $\mu(\lambda)$ values for three radiation doses.

On the other hand, assuming that the radiation monitor results are correct, the two sets of spectra can be used to determine $\mu(\lambda)$. Three values of radiation dose have been used to determine $\mu(\lambda)$ and are presented in table B.4. The determined $\mu(\lambda)$ values are about a factor of three to four different than the values determined by Kirsebom and Sollie (table B.3). One does not expect the lead-glasses to be that different; the dosage determined from the radiation monitors is probably an overestimate.

Assuming that $\mu(\lambda)$ values of Kirsebom and Sollie are correct, the expected damage to the lead-glass samples on the calorimeter can be calculated. A 3% to 5% change of the transmittances for the wavelengths between 350 nm and 420 nm is expected after a 100 rad dose. The spectrophotometer is capable of showing this change in transmittance. A difference has not been seen and possible explanations, as indicated above, are either (i) the radiation monitor has overestimated the dose or (ii) instant bleaching.

Cycle Number	Exposure Time (min) Period	Cumulative
1	15	15
2	15	30
3	30	60
4	60	120
5	180	300
6	180	480
7	180	660
8	360	1020
9	360	1380

Table B.5: The exposure time periods and cumulative time that the two lead-glass samples were exposed to sunlight.

B.4 Curing

Physics practice has been to expose irradiated lead-glass to sunlight for curing. The estimated recovery time from radiation damage for lead-glass is estimated to be 50 years [85] (from measurements over a period of 1.5 years of lead-glass not exposed to light). During May 1991, the two most irradiated lead-glass samples were exposed to sunlight for different time periods. Two non-irradiated lead-glass samples were also exposed to the sunlight as controls. Table B.5 shows the exposure time periods and cumulative times; the uncertainty of the time of exposure is a few minutes. The exposure periods were scattered over a few weeks whenever there was not a threat of rain; some of the exposure periods were while the sky was overcast.

The never-irradiated lead-glass samples spectra showed no changes and continually showed that the reproducibility of the spectrophotometer results. Figure B.3 shows the radiation damaged transmission spectrum and the spectra after seven of the

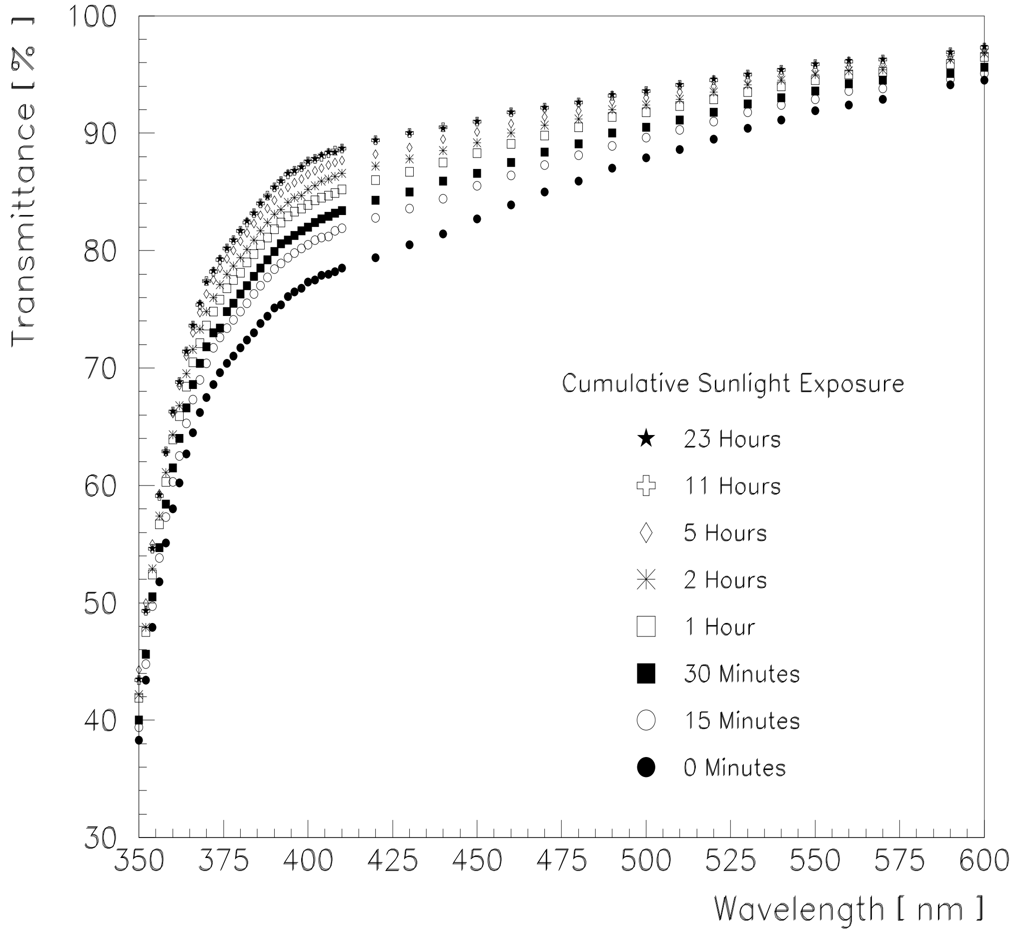

Figure B.3: The transmission spectra after different exposure periods (different cumulative times) as the lead-glass sample cures. The 11 and 23 hour cumulative time spectra are nearly the same, and the symbols are not resolved.

curing periods for one of the lead-glass samples. The spectra after 11 and 23 hours of cumulative exposure to sunlight are nearly the same. The spectra of figure B.3 have been normalized by the transmission spectrum taken before radiation exposure. These normalized spectra, as shown in figure B.4, show the loss of transmittance due to the radiation damage and the subsequent recovery due to exposure to sunlight. Complete recovery would be a value of 1.0 corresponding to no difference from

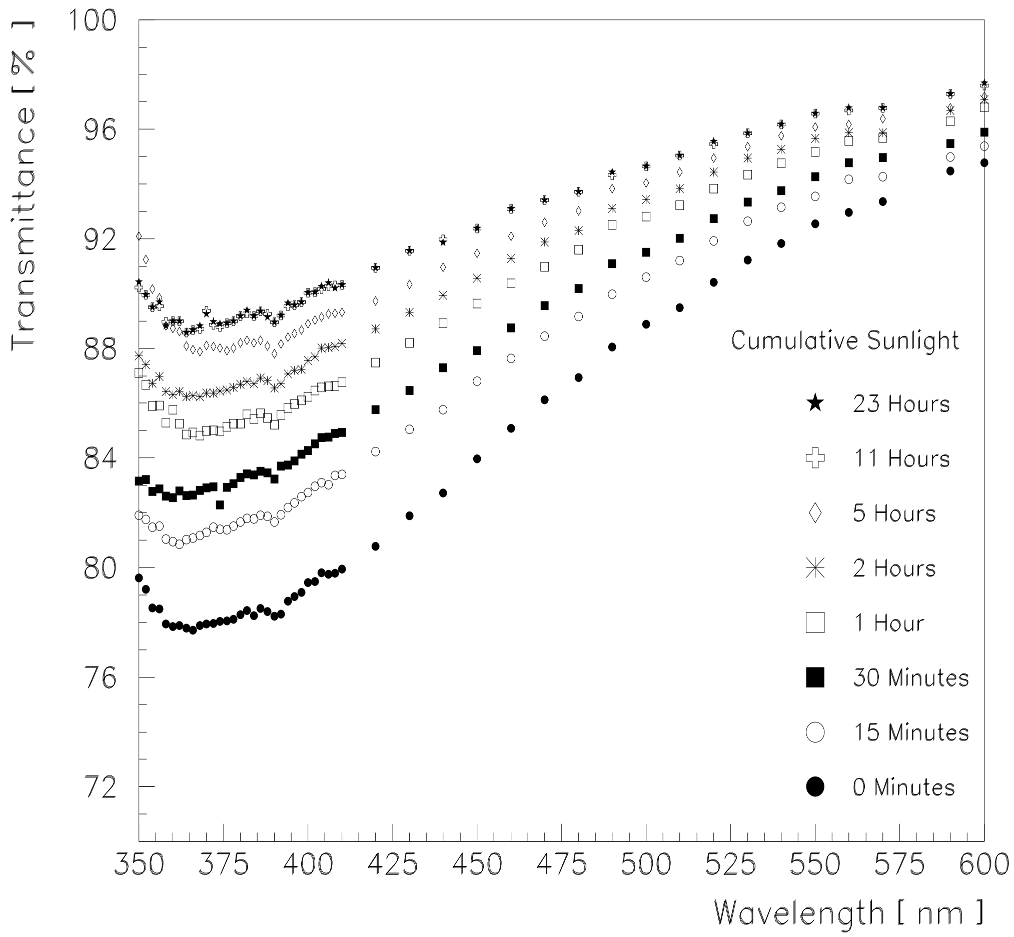

Figure B.4: The loss of transmittance due to the radiation damage and the recovery due to exposure to sunlight. The transmission spectra after different exposure periods (different cumulative times) as the lead-glass sample cures, normalized by the non-irradiated spectrum. The 11 and 23 hour cumulative time spectra are nearly the same, and the symbols are not resolved.

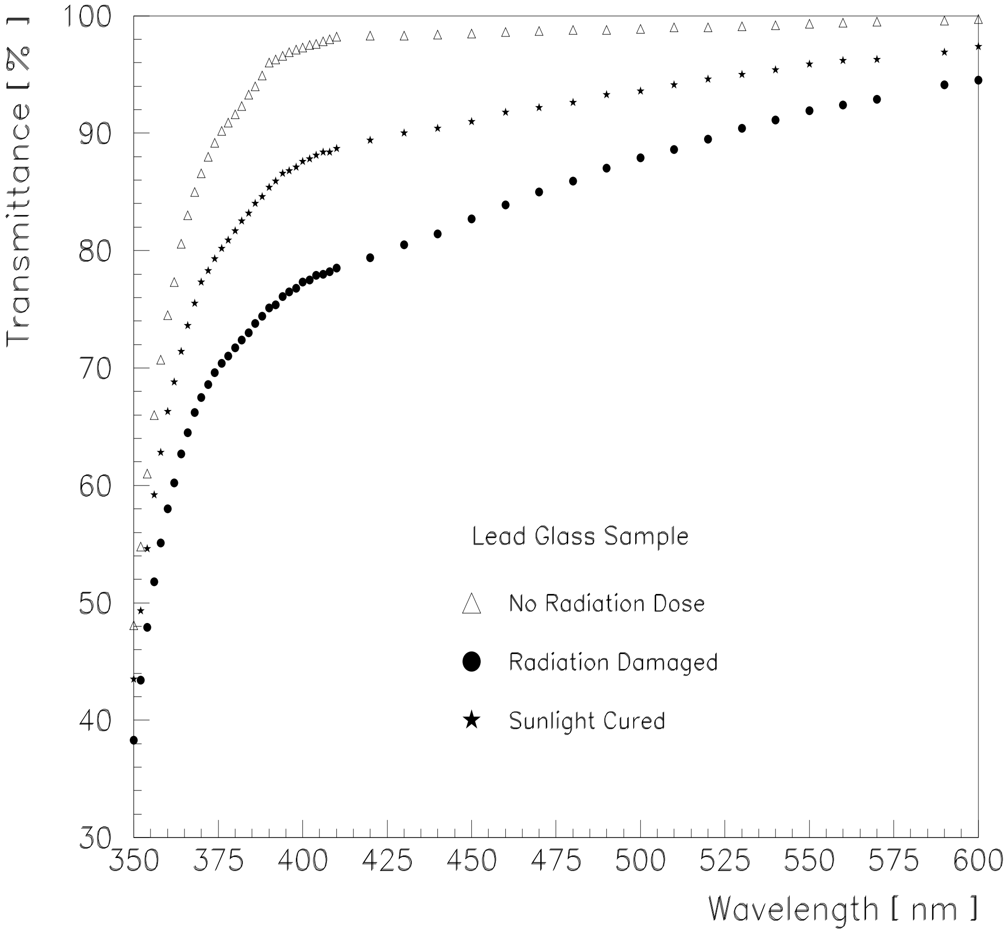

Figure B.5: The transmission spectra of a lead-glass sample before irradiation, radiation damaged and after sunlight exposure (cured).

the non-irradiated transmission spectrum. After 23 hours of exposure to sunlight, the lead-glass sample's transmittances have not shown any more recovery. The non-irradiated, radiation damaged and cured transmission spectra are shown in figure B.5. The sunlight curing does not cause a complete recovery of the transmittance.

The first hour of exposure to sunlight appears to have the greatest effect. Figure B.6 shows the transmittance normalized by the non-irradiated transmittance

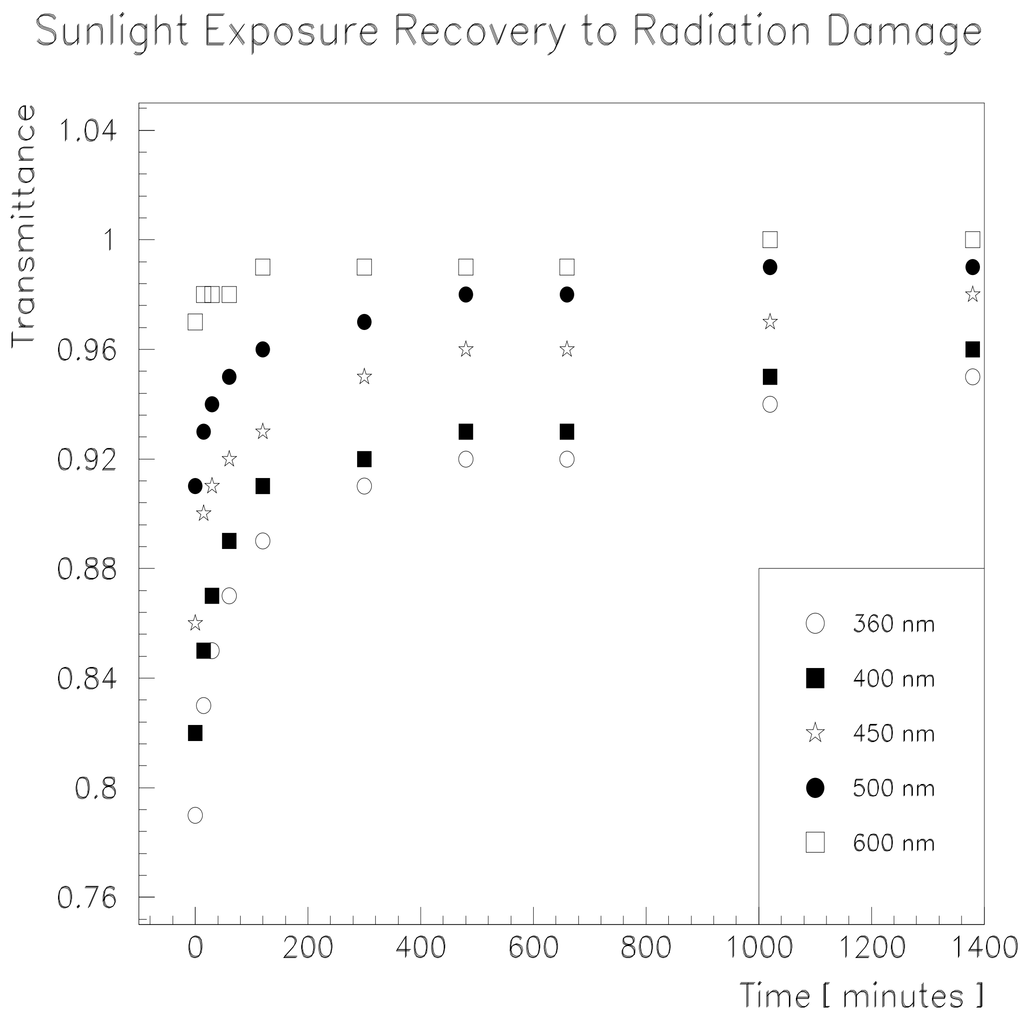

Figure B.6: The transmittance of several wavelengths while curing as a function of cumulative sunlight exposure time.

as a function of exposure time to sunlight for five wavelengths. The curing rate does not appear to be a function of wavelength.

B.5 Discussion

The spectrophotometer has been used to monitor radiation damage to the central calorimeter. The lead-glass samples placed about the central calorimeter have not shown any degradation of the transmission spectrum.

Two lead-glass samples were irradiated about a factor of 10 more than the lead-glass samples about the calorimeter. The two lead-glass samples showed radiation damage. There appears to be a discrepancy between the radiation dose received when using radiation damage parameters from a published experiment and the radiation monitors. The radiation monitors may be overestimating the dose, due to uncertainty about the type of radiation, by a factor of 2 to 5.

The two most irradiated lead-glass samples have been partially cured by exposure to sunlight. The sunlight curing does not cause the transmission spectrum to recover fully; the recovery leads to transmittances 94% of before-irradiation at ultraviolet wavelengths to nearly 100% for the green part of the spectrum. A single central calorimeter counter Monte Carlo simulation (Appendix C) shows that the photoelectron signal should decrease by 18% for a 1 GeV incident gamma ray when using Kirsebom and Sollie's parameterization of the radiation damage and assuming a 100 rad dose. Since no large decrease in signal output has been observed, it is probable that the radiation monitors associated with the central calorimeter have overestimated the radiation dose.